PALoc: Advancing SLAM Benchmarking With Prior-Assisted 6-DoF Trajectory Generation and Uncertainty Estimation

Xiangcheng Hu, Linwei Zheng, Jin Wu, Ruoyu Geng, Yang Yu, Hexiang Wei, Xiaoyu Tang, LuJia Wang, Jianhao Jiao and Ming Liu

香港科技大學 THE HONG KONG UNIVERSITY OF SCIENCE AND TECHNOLOGY

ICRA2024 YOKOHAMA | JAPAN

Introduction

Accurate ground truth (GT) trajectories are vital for SLAM evaluation, especially in complex environments. However, existing methods face challenges such as limited coverage, occlusion, and inability to handle degenerate scenarios. PALoc is a novel prior map-assisted approach that generates dense and high-precision 6-DoF GT trajectories across diverse scenarios. It provides detailed pose uncertainty analysis and open-sourced toolbox for map evaluation. Experiments show significant improvements in accuracy and robustness across diverse environments.

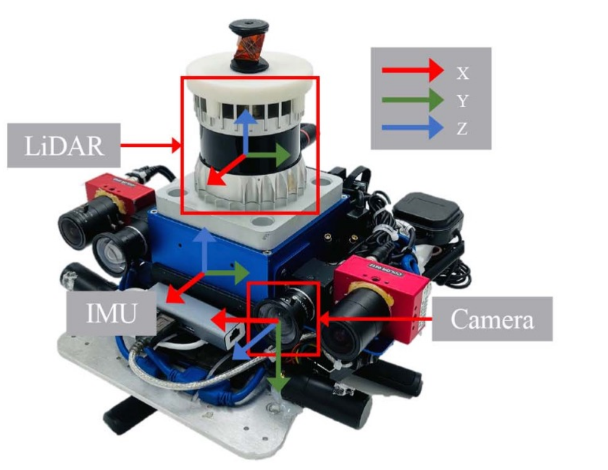

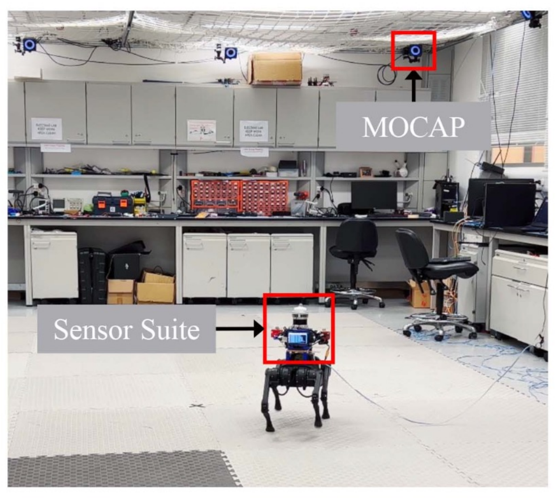

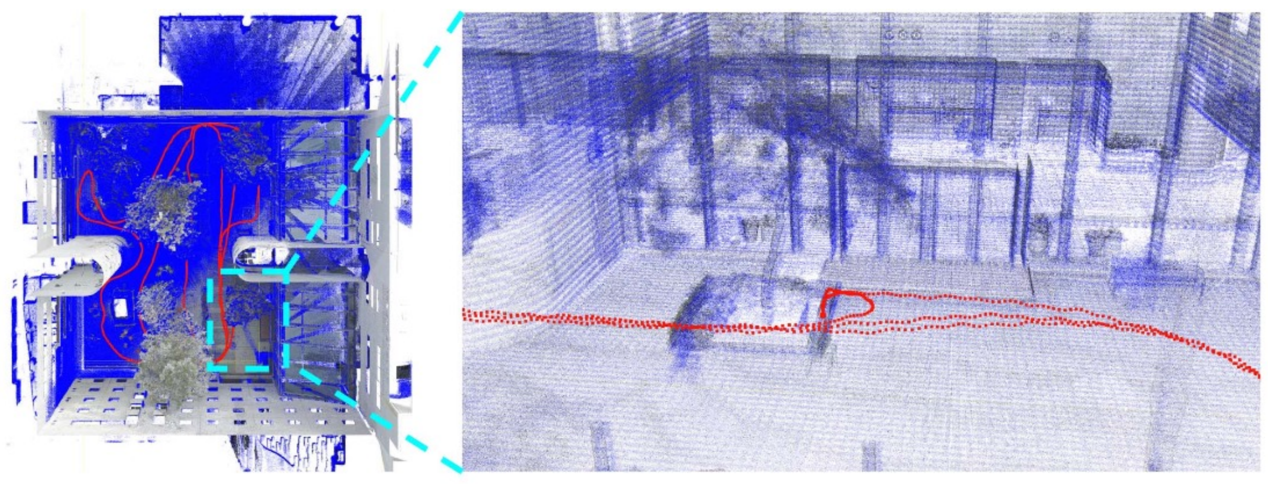

Methodology

- The first localization system for dense 6-DoF ground truth trajectory generation for SLAM benchmarking.
- Comprehensive uncertainty propagation analysis.
- Map evaluation for indirect trajectory assessment.

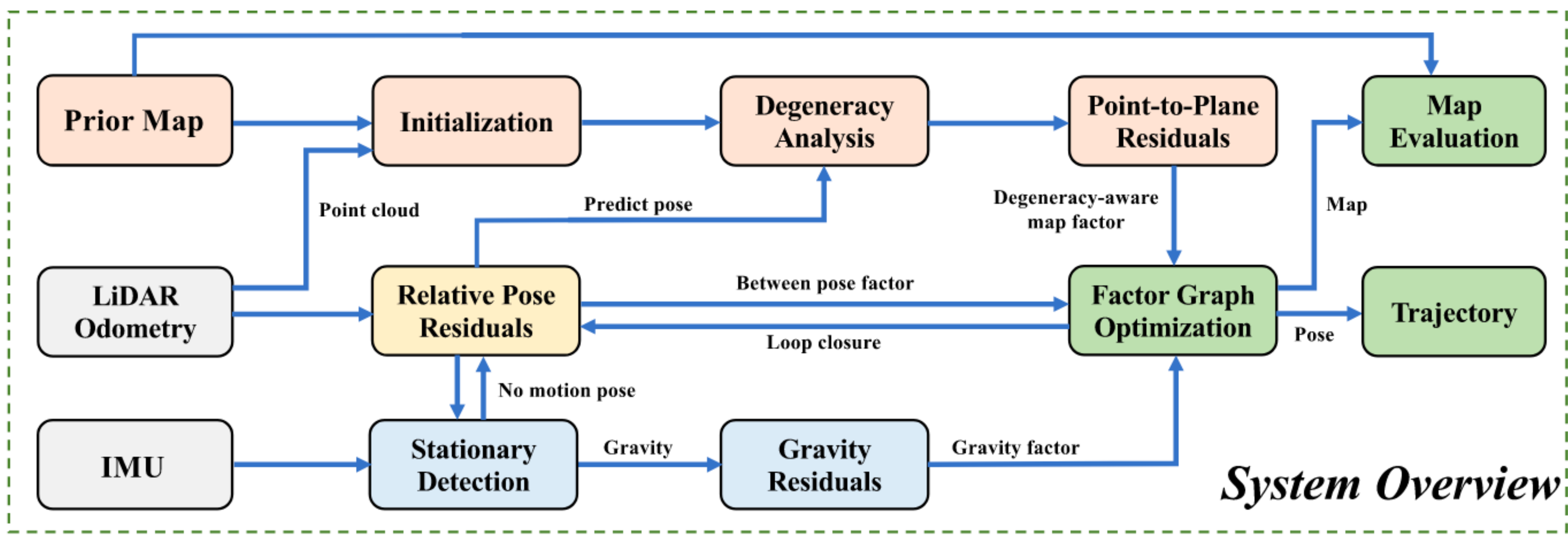

Fig. 2. System pipeline overview. This figure illustrates the architecture of our system, starting with initialization on a prior map and LiDAR odometry. Degeneracy analysis and point-to-plane registration are employed to create a degeneracy-aware map factor. The system also processes odometry and IMU data for stationary detection, forming no motion factors, and integrating gravity factors. Following the optimization of the factor graph on a framewise basis, loop closure detection is carried out, contributing to the loop factor. This sequential pipeline results in the generation of estimated poses and maps, which assists in the indirect evaluation of trajectory accuracy.

Conclusion

PALoc enhances SLAM evaluation and expands its applicability in robotics research.

X. Hu *et al.*, "PALoc: Advancing SLAM Benchmarking With Prior-Assisted 6-DoF Trajectory Generation and Uncertainty Estimation," in *IEEE/ASME Transactions on Mechatronics*, doi: 10.1109/TMECH.2024.3362902.

Experiments

TABLE I
QUANTITATIVE COMPARISON OF ATE [CM] AND RPE [CM] ACROSS DIVERSE ENVIRONMENTS AND PLATFORMS USING DIFFERENT FRONT-END ODOMETRY METHODS (PLS AND PFL2)

Sequence	**PLS**		**PFL2**	
	ATE ↓	**RPE ↓**	**ATE ↓**	**RPE ↓**
Handheld Indoor				
MCR_slow	5.70	3.89	7.36	2.49
MCR_normal	7.71	4.95	10.12	3.78
Quadruped Robots Indoor				
MCR_slow_00	2.00	0.90	3.73	0.54
MCR_slow_01	2.93	1.51	2.81	0.70
MCR_normal_00	3.96	2.49	5.00	0.72
MCR_normal_01	3.58	0.93	5.23	0.88
Handheld Outdoor				
parkinglot_01*	–	–	26.10	3.06
redbird_01	–	–	9.98	1.34
redbird_02	–	–	10.32	1.34

* Degenerate scenarios. A dash (–) indicates sequences that were not tested.

TABLE II
MAPAC [CM] AND CD COMPARISON FOR 20-CM THRESHOLD IN DIVERSE ENVIRONMENTS

Sequence	LM		LS		FL2		ICP		HDL		FL2L		PFL2	
	AC ↓	CD ↓	AC ↓	CD ↓	AC ↓	CD ↓	AC ↓	CD ↓	AC ↓	CD ↓	AC ↓	CD ↓	AC ↓	CD ↓
Handheld Outdoor														
garden_day	4.14	7.95	3.94	7.87	5.98	10.73	3.64	7.27	6.06	10.65	<u>3.50</u>	<u>7.20</u>	**3.48**	**7.03**
garden_night	4.36	8.08	3.92	7.83	5.91	10.78	<u>3.23</u>	<u>7.06</u>	6.12	10.71	3.52	7.23	**3.19**	**6.99**
canteen_day	5.65	9.45	5.48	9.24	6.32	10.51	<u>4.86</u>	<u>8.23</u>	6.59	10.63	5.59	9.02	**4.71**	**8.08**
canteen_night	5.60	9.60	5.29	9.61	6.77	10.87	<u>5.07</u>	<u>8.42</u>	6.93	10.96	5.56	8.94	**4.76**	**8.16**
Handheld Indoor														
escalator_day	5.40	9.10	8.65	15.09	6.92	10.36	×	×	7.66	11.28	<u>4.29</u>	<u>7.51</u>	**3.88**	**7.13**
building_day	10.11	19.05	7.65	15.01	6.68	12.63	6.72	8.54	7.11	11.35	<u>4.19</u>	<u>7.88</u>	**4.14**	**7.49**
corridor_day*	7.40	13.14	6.24	12.51	7.28	12.91	×	×	8.08	11.59	5.59	8.44	**3.99**	**5.79**
MCR_slow	7.66	13.84	<u>4.08</u>	6.54	6.19	8.55	**3.96**	**5.92**	×	×	×	×	4.63	<u>6.52</u>
MCR_normal	4.28	7.92	<u>3.85</u>	<u>7.01</u>	×	×	×	×	×	×	×	×	**3.71**	**5.86**
dynamic_02	9.58	18.07	9.78	18.49	9.63	17.98	<u>4.13</u>	<u>8.09</u>	7.44	10.96	4.62	8.34	**4.06**	**7.82**
dynamic_04	9.66	18.25	9.81	18.28	9.68	18.00	<u>4.30</u>	<u>7.90</u>	4.35	11.36	5.06	8.42	**4.20**	**7.67**

* Degenerate scenarios. × signifies a failure of the algorithm on the respective datasets. **Bold** indicates the best accuracy, <u>underline</u> indicates the second best.

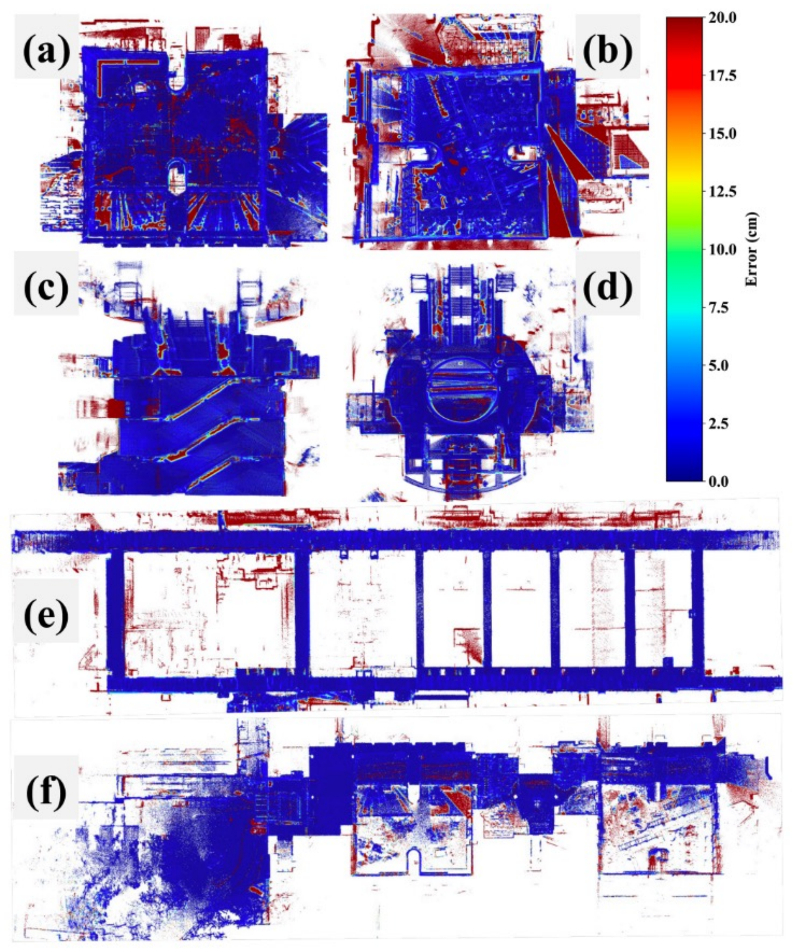

Fig. 4. Error map of diverse campus scenes. The degree of color transition from blue to red indicates an increasing error in the mapped area. (a) `garden_day` (259.5 m). (b) `canteen_day` (253.1 m). (c) XZ view of `escalator_day` (600.1 m). (d) XY view of `escalator_day` (600.1 m) with ceiling removal. (e) `corridor_day` (656.4 m). (f) `building_day` (717.8 m).

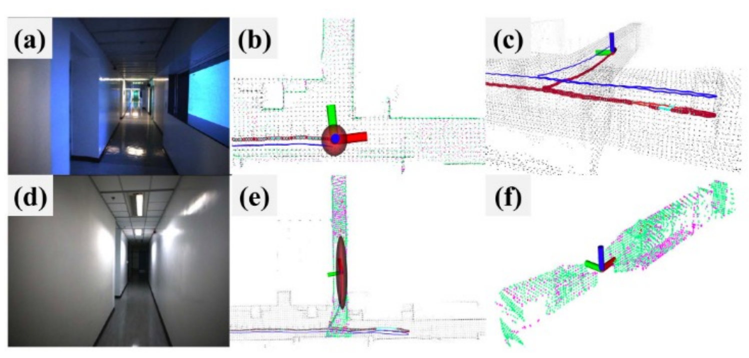

Fig. 5. Translation degeneracy analysis in corridor. (a) and (d) represent real-world corridor scenes. The black point cloud represents the prior map, and the red sphere with coordinate axes represents the relative constraint strength in the XYZ dimensions but is unrelated to the overall size of the ellipsoid. The flatter the ellipsoid, the more severe the degeneration in a specific dimension. The blue and light blue trajectories and the red points on the trajectories represent the FL2 odometry trajectory, our algorithm trajectory, and the pose with DM constraints. Our algorithm eliminates Z-axis drift error while ensuring robustness in a U-turn intersection (c). The point clouds of different colors in (f) indicate the corresponding number of constraints in XYZ dimensions (see Section VI-B).

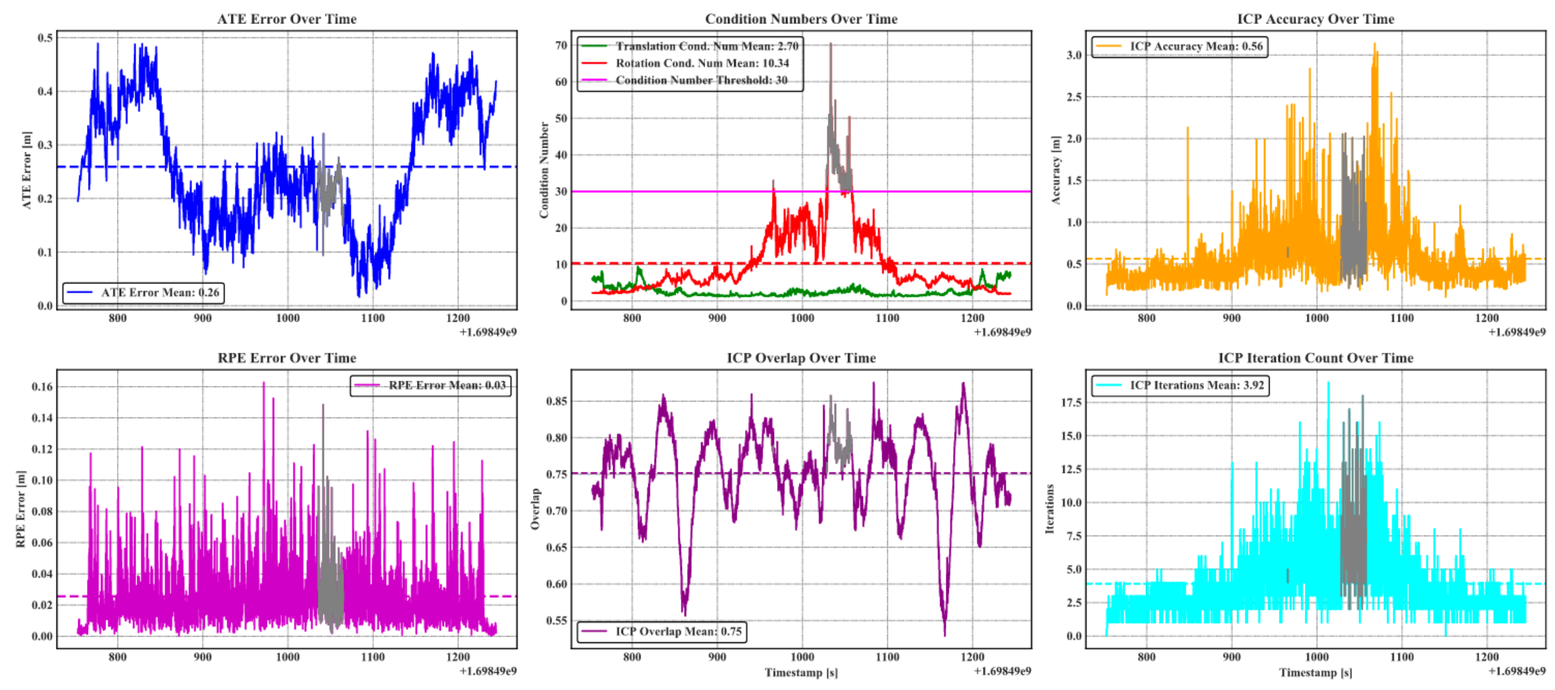

Fig. 6. Degeneracy scenario analysis. The figure provides a detailed analysis of the DM factor in PALoc, applied to the `parkinglot_01` dataset with yaw degeneracy. It includes a time-variant depiction of ATE, ICP accuracy, ICP iteration count, ICP overlap rate, and the condition numbers for translation and rotation. A specific threshold for the condition number, marked by the gray area, is set to identify degeneracy. It is observed that during rotational degeneracy in the scene, there is a notable decline in ICP accuracy, and ICP overlap rate, along with a significant increase in ICP iteration counts. These observations align well with the actual scenarios encountered in the parking lot setting.

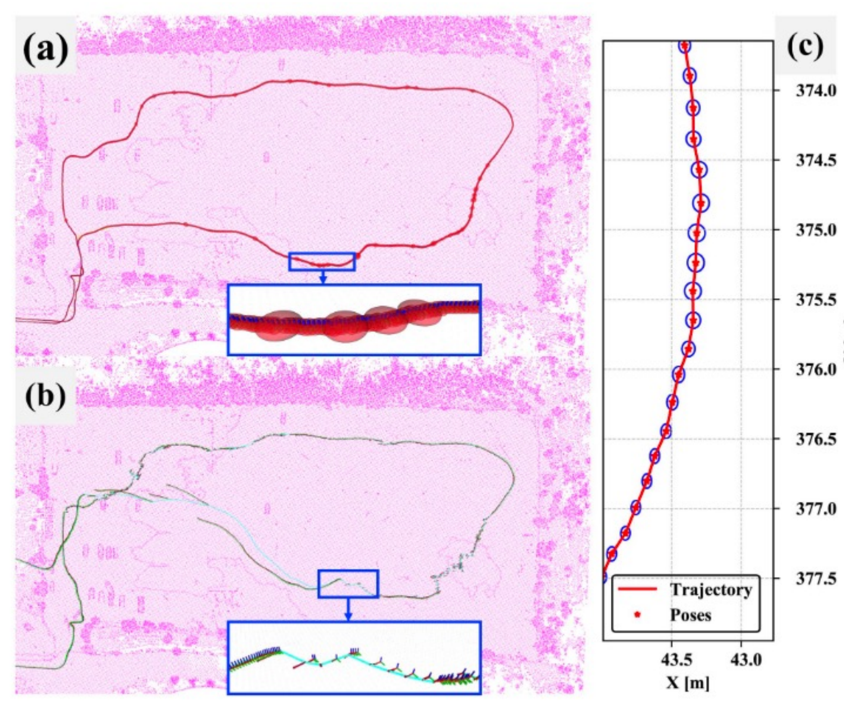

Fig. 7. Trajectory comparison and uncertainty visualization in rotation degenerate parking lot. (a) Robust performance of the PFL2 under conditions of rotational degeneracy, operating smoothly. Red spheres indicate the uncertainty in the translation part; larger spheres denote greater uncertainty, with reduced uncertainty along the Z-axis. Occasional large covariance spheres represent severe degeneracy causing matching errors, leading to the exclusion of these map factors. (b) Trajectory of FL2L in blue, with coordinate axes representing the poses, clearly showing direct localization failure in scenarios with rotational degeneracy. (c) Pose uncertainty in the X and Y dimensions at a 95% confidence; due to the scale of the visualization, the uncertainty in Y is almost comparable to X, aligning with the observed real-world scenario.

TABLE III
ABLATION STUDY OF ATE [CM], RPE [CM], AND AC [CM] ON MCR_NORMAL_00

Method	**ATE ↓**	**RPE ↓**	**AC ↓**
FL2	9.80	1.20	5.47
w/o LO	22.3	4.93	7.71
w/o DM	9.61	1.10	5.86
w/o LC	5.47	<u>0.96</u>	5.38
w/o NM	5.38	1.58	4.11
w/o GF	<u>5.03</u>	1.19	4.06
All	**5.00**	**0.72**	**3.93**

Bold indicates the best performance; <u>underlined</u> signifies the second-best.